Journal of Alloys and Compounds 498 (2010) 107–112

Contents lists available at ScienceDirect

Journal of Alloys and Compounds

journal homepage: www.elsevier.com/locate/jallcom

Synthesis of nanocrystalline Ni_3Al by mechanical alloying and its microstructural characterization

Youjun Yu[a,b], Jiansong Zhou[a], Jianmin Chen[a,*], Huidi Zhou[a], Chun Guo[a,b], Baogang Guo[c]

[a] State Key Laboratory of Solid Lubrication, Lanzhou Institute of Chemical Physics, Chinese Academy of Sciences, Lanzhou 730000, People's Republic of China
[b] Graduate School, Chinese Academy of Sciences, Beijing 100039, People's Republic of China
[c] Analytical and Testing Center, Southwest University of Science and Technology, Mianyang 621010, People's Republic of China

ARTICLE INFO

Article history:
Received 24 November 2009
Received in revised form 11 March 2010
Accepted 13 March 2010
Available online 18 March 2010

Keywords:
Nanocrystalline
Ni_3Al
Intermetallic
Mechanical alloying
Characterization

ABSTRACT

Nanocrystalline Ni_3Al intermetallic compound was successfully synthesized by mechanical alloying of the mixed powders of elemental Ni and Al. The phase evolution and microstructural changes of the powders during mechanical alloying were investigated by means of X-ray diffraction, field-emission scanning electron microscopy, transmission electron microscopy, and energy dispersive spectrometry. It was found that supersaturated Ni(Al) solid solution was formed during the early stage of mechanical alloying process. Upon further milling, Ni(Al) solid solution was transformed into ordered Ni_3Al intermetallic nanocrystalline. It is imperative to adopt a long enough ball milling time (120 h in the present work) so as to ensure the complete transformation of Ni(Al) solid solution to Ni_3Al intermetallic nanocrystalline and the formation of well ordered Ni_3Al nanocrystals composed of fine grains with a size of about 11 nm.

1. Introduction

Ni_3Al intermetallic compound exhibits excellent physical and mechanical properties, such as high melting temperature, high hardness, low density, and good corrosion and oxidation resistance at an elevated temperature [1–4]. Furthermore, the yield strength of Ni_3Al intermetallic, instead of decreasing with increasing temperature, shows an anomalous increase at intermediate temperatures of about 600–800 °C [4–6]. Thanks to the excellent physical and mechanical properties, Ni_3Al intermetallic compound may be promising high temperature structural material and corrosion resistant material for gas turbine hardware, high temperature dies and molds, cutting tools and heat treatment fixtures [4–7]. However, its application as engineering materials is highly restricted by the extremely high brittleness of polycrystalline Ni_3Al at ambient temperature [8,9] and poor workability as well. A number of attempts have been made to overcome this drawback. For example, Liu et al. prepared Ni_3Al with a tensile ductility of 40–50% by doping 0.04 wt.% boron [9–11]. McFadden et al. found that Ni_3Al nanocrystalline subjected to severe plastic deformation showed increased ductility [12], which might be closely dependent on the small size effect and high surface area and activity resulting in improved physical and mechanical properties of the nanocrystallines [6,12–15]. This implies that the scope of Ni_3Al intermetallic compound as a structural material in engineering may be effectively broadened by inducing nanocrystallization leading to increased toughness. Mechanical alloying (MA) is one of the most commonly used methods for such a purpose [16–19]. For instance, nanocrystalline alloy Ni–25% Al (at.%) has been synthesized by way of the mechanical alloying of the mixed powders of relevant elements [20,21], or by way of the mechanical alloying of nickel aluminides such as AlNi, Al_3Ni, and Al_3Ni_2 mixed with Ni powders in association with subsequent heat-treatment like hot-pressing consolidation [22–24]. These studies have helped to shed light on the interaction mechanisms of solid phase components during mechanical alloying. However, MA is still facing some uncertainty concerning the synthesis of Ni_3Al. Cardellini reported that supersaturated solid solution Ni(Al) was the only product during MA process [20]. Enayati et al. found that MA initially resulted in a Ni(Al) solid solution which was transformed to disordered Ni_3Al intermetallic compound with nanocrystalline structure on further milling [21]. Krasnowski et al. reported that the ordering of Ni(Al) solid solution was the only product at the first stage of the MA process, then Ni(Al) solid solution was transformed into ordered Ni_3Al intermetallic compound during heating of the milled products in calorimeter [22–24].

In the present study, nanocrystalline Ni_3Al intermetallic compound was synthesized by mechanical alloying. The phase transformation and microstructural evolution occurring in MA process were investigated. The average grain size and mean

* Corresponding author. Tel.: +86 931 4968018.
E-mail address: chenjm@lzb.ac.cn (J. Chen).

0925-8388/$ – see front matter © 2010 Elsevier B.V. All rights reserved.
doi:10.1016/j.jallcom.2010.03.123

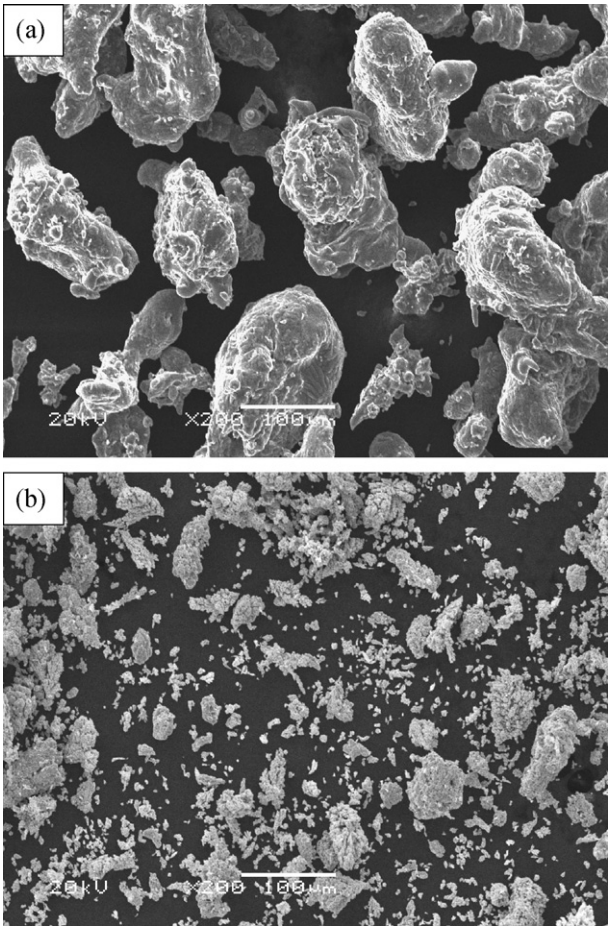

Fig. 1. SEM micrographs of mixed powders of elemental (a) Al and (b) Ni.

lattice strains of the powders after mechanical alloying were estimated based on X-ray diffraction (XRD) analysis and field-emission scanning electron microscopic (SEM) and transmission electron microscopic (TEM) observation.

2. Experimental

Powder mixtures of elemental Al (30–150 μm, 99.5% purity) and Ni (about 75 μm, 99.0% purity) with an atomic composition (at.%) of Ni–25% Al were used as starting materials, whose SEM images are shown in Fig. 1. As it can be seen in Fig. 1a and b, Al particles have an irregular shape, while Ni particles have a cauliflower-like shape or an irregular flocculent shape.

Mechanical alloying was performed under argon atmosphere at room temperature using a high energy vario-planetary ball mill (Fritsch Pulverisette P-4) with tungsten carbide vials and balls. The ball-to-powder weight ratio is 6:1 and the rotation speed of vial is 500 rpm. The milling was interrupted at selected intervals and a small amount of the corresponding milled powders was collected for characterizations.

The phase transformation and microstructural changes of the powders were investigated using an X'Pert-MRD X-ray diffractometer (XRD, Philips; Cu Kα radiation, λ = 0.1541 nm). The average grain size and mean lattice strain of the powders were also calculated by taking into account the broadening of the XRD peaks, which is attributed to crystalline refinement and lattice strain as well as instrumental broadening. The instrumental broadening was determined using a Si standard and subtracted from the experimental breadth to obtain the physical broadening of each diffraction line which was then used for calculating grain size and lattice strain. Since the XRD broadening at low angles is dominated by small grain sizes and by internal strains at high angles [25], the low angle reflections were used to calculate the average grain size based on the Scherrer formula [26], and the high angle reflections to estimate the mean lattice strain based on Stokes and Wilson formula [27]. Similar practices have been reported by Enayati et al. [21] and Shaw et al. [28] in calculation of the average grain size using Scherrer formula. Briefly, the (1 1 1) and (2 0 0) reflections of fcc-Ni were considered in calculating the average grain size of Ni(Al) solid solution, and those of Ni_3Al considered in estimating the average grain size of

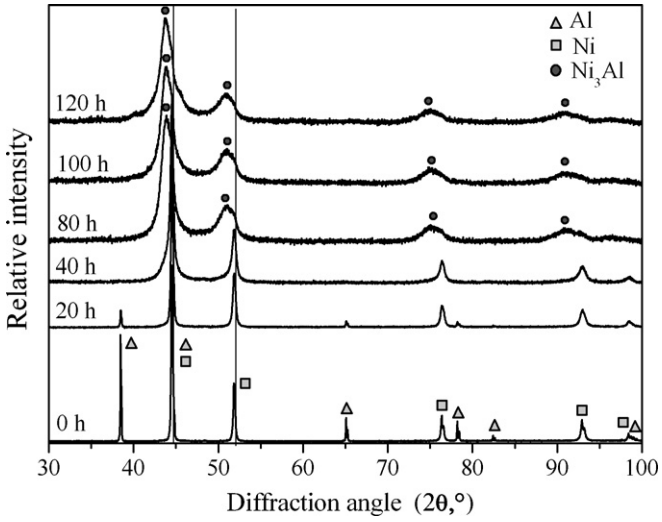

Fig. 2. XRD patterns of Ni–Al powder mixture before and after various milling times.

Ni_3Al intermetallic compound, based on Scherrer formula shown in Eq. (1).

$$\beta(2\theta) = \frac{0.9\lambda}{D\cos\theta} \quad (1)$$

where β is the full width at half maximum of the XRD peaks, θ is the Bragg diffraction angle, λ is the wavelength of the X-ray radiation, D is the average grain size. Similarly, the mean lattice strain of Ni(Al) solid solution was calculated by considering the (2 2 0) and (3 1 1) reflections of fcc-Ni, and that of Ni_3Al intermetallic compound was calculated by taking into account the (2 2 0) and (3 1 1) reflections of Ni_3Al, based on the Stokes and Wilson formula shown in Eq. (2).

$$\beta(2\theta) = 2\varepsilon\tan\theta \quad (2)$$

where β is the full width at half maximum of the XRD peaks, θ is the Bragg diffraction angle, ε is the mean lattice strain.

The morphology of the powders was observed at an acceleration voltage of 20 kV using a JSM-5600LV field-emission scanning electron microscope (FESEM, JEOL, Japan) equipped with an energy-dispersive spectrometer (EDS). The average grain size, crystal structure and chemical composition of the milled particles were analyzed at an accelerating voltage of 200 kV using a JEM-2010 high resolution transmission electron microscope (HRTEM, JEOL, Japan). TEM specimens were prepared by mixing the powders in a small amount of ethanol and follow-up mounting of the mixture onto a copper grid. For a comparison, the elemental composition of the powders collected at various milling time was also analyzed using an energy-dispersive spectrometer attached to TEM.

3. Results and discussions

The XRD patterns of the mixed powders of Ni–25% Al (at.%) before milling and after milling for different durations are shown in Fig. 2. For the mixed powders before milling, very sharp peaks of Ni and Al are visible, which imply that the as-received mixed powders may have very fine crystalline size. After being milled for 20 h, broadening of the XRD peaks of Ni and Al is observed but no peaks of Ni_3Al is visible, which indicates that the mixed powder had been aggregated to some extent leading to increased lattice strain at this milling time but did not experience mechanical alloying thereat. After 40 h milling, the XRD peaks of Al disappear, and those of Ni shift toward lower angles. This implies that, during the milling process, Al atoms with a larger size had been dissolved into Ni lattice forming Ni(Al) solid solution with a structure the same as that of fcc-Ni but having a slightly larger lattice parameter than Ni. The average grain size of Ni(Al) after 40 h of milling, estimated using the Scherrer formula, is about 61 nm, while the mean lattice strain, ε, estimated using the Stokes and Wilson formula, is about 0.35%. Increasing milling time to 80 h results in disappearance of Ni peaks, while Ni_3Al peaks begin to appear, which indicates that crystalline Ni_3Al intermetallic compound had been formed via mechanical alloying after 80 h of milling. Further milling up to 120 h

Table 1
Experimental materials, experimental method and corresponding products, grain size (D) and lattice strain (ε) obtained in present paper and other literatures.

	Experimental materials	Experimental method and corresponding products		D (nm)		ε (%)	
		MA	MA[a]	MA	MA[a]	MA	MA[a]
Present work	Al and Ni powders	After 40 h milling Ni(Al) solid solution		61		0.35	
		After 80 h milling ordered Ni_3Al intermetallic		22		1.02	
		After 100 h milling ordered Ni_3Al intermetallic		12		1.19	
		After 120 h milling ordered Ni_3Al intermetallic		11		1.22	
Other work							
[21]	Al and Ni powders	After 10 h milling Ni(Al) solid solution					
		After 20 h milling disordered Ni_3Al intermetallic					
		After 80 h milling disordered Ni_3Al intermetallic		10			
[23]	AlNi intermetallic and Ni powder	After 15 h milling Ni(Al) solid solution	Hot-pressing consolidation ordered Ni_3Al intermetallic	12	23		0.06
	Al_3Ni_2 intermetallic and Ni powder	After 15 h milling Ni(Al) solid solution	Hot-pressing consolidation ordered Ni_3Al intermetallic	12	21		0.07
[24]	Al_3Ni intermetallic and Ni powder	After 10 h milling Ni(Al) solid solution	Hot-pressing consolidation ordered Ni_3Al intermetallic	16	31	0.73	0.05
	$Ni_{96}Al_4$ solid solution and Al powder	After 15 h milling Ni(Al) solid solution	Hot-pressing consolidation ordered Ni_3Al intermetallic	19	32	0.93	0.08

[a] MA and subsequent heating process.

leads to no obvious changes of the XRD patterns as compared with milling for 80 h.

The average grain size and lattice strain of Ni(Al) solid solution and Ni_3Al intermetallic compound, estimated using the Scherrer formula and Stokes and Wilson formula by taking into account the broadening of XRD peaks, are listed in Table 1. These values reported earlier in the literatures [21–24] are also given in Table 1. In addition, the experimental materials, experimental method and corresponding products are listed in this table for explicit comparison. In combination with the XRD results, it can be inferred that the Ni_3Al intermetallic compound formed after 80 h of milling has a grain size of 22 nm and a lattice strain of 1.02%. Increasing milling time to 100 h and 120 h leads to no further structural changes of the XRD patterns as compared with milling for 80 h, which indicates that the steady-state stage of MA process is reached and the final product of these processes is the crystalline Ni_3Al intermetallic compound. After 100 h of milling time, the average grain size and the mean lattice strain of Ni_3Al are 12 nm and 1.19%, respectively. These values after 120 h of milling time are 11 nm and 1.22%, respectively. It can be seen from Table 1 that, comparing present paper with the literature [21], the experimental materials are the same such as Al and Ni powders and the product formed in the early stage of milling operation is the same such as Ni(Al) solid solution during mechanical alloying process. With increasing of the milling time, both our present work and the literature [21] inferred that Ni(Al) solid solution transformed into Ni_3Al intermetallic compound via Ni diffusion due to the accumulation of internal strain and refinement of grains associated with extended milling. Although the Ni_3Al intermetallic compound has a similar grain size about 10 nm, the Ni_3Al phase obtained in literature [21] has a disordered structure, while the Ni_3Al phase obtained in our present work has an ordered structure. At the same time, as given in Table 1, the experimental materials used in the literatures [23,24] are obviously different from those used in present paper and the literature [21]. It can be noticed that the Ni(Al) solid solution was the only product during MA process, then the Ni(Al) solid solution transformed into an ordered Ni_3Al intermetallic compound after subsequent heating process such as hot-pressing consolidation [23,24]. While the ordered Ni_3Al intermetallic compound was directly formed by MA process in present work. In spite of the differences in grain size (D) and lattice strain (ε) between present paper and the literatures [23,24], which may be attributed to the experimental materials as well as experimental method, a common feature exists in both cases, namely, a larger grain size (D) associating with a smaller lattice strain (ε).

The 2θ values corresponding to characteristic diffraction peaks of Ni_3Al formed after 120 h of mechanical alloying and that in JCPDS files are listed in Table 2. It can be seen that the 2θ values of the Ni_3Al prepared in the present work agree well with that in JCPDS files [29], and the slight difference in comparison with the JCPDS files might arise from the broadening of the XRD peaks of the sample after full mechanical alloying.

The SEM images of the mixed powders after milling for 40 h, 80 h, and 120 h are shown in Fig. 3, and the atomic composition of the relevant powder samples, determined by using EDS, is listed in Table 3. After 40 h of milling, the powders appear as equiaxial particles and have an average size of about 3 μm (see Fig. 3a). The magnified image (see Fig. 3b) indicates that the equiaxial particles have a homogeneous multi-layered structure due to the repeated action of cold welding and fracturing of the powder particles during MA process [6]. EDS analysis shows that the equiaxial particles are rich in Ni and contain a small amount of elemental Al, with a nominal composition of about 97.06% Ni and 2.94% Al. Such an atomic composition of the milled powder samples agrees well with rele-

Table 2
The 2θ (°) values with related diffraction plane of Ni_3Al phase formed after 120 h of mechanical alloying and the corresponding values in JCPDS flies [29].

Diffraction plane	2θ value (°)	
	After 120 h of milling	JCPDS
(1 1 1)	43.797	43.604
(2 0 0)	50.912	50.703
(2 2 0)	75.008	75.022
(3 1 1)	90.350	91.212
(2 2 2)	96.263	96.558

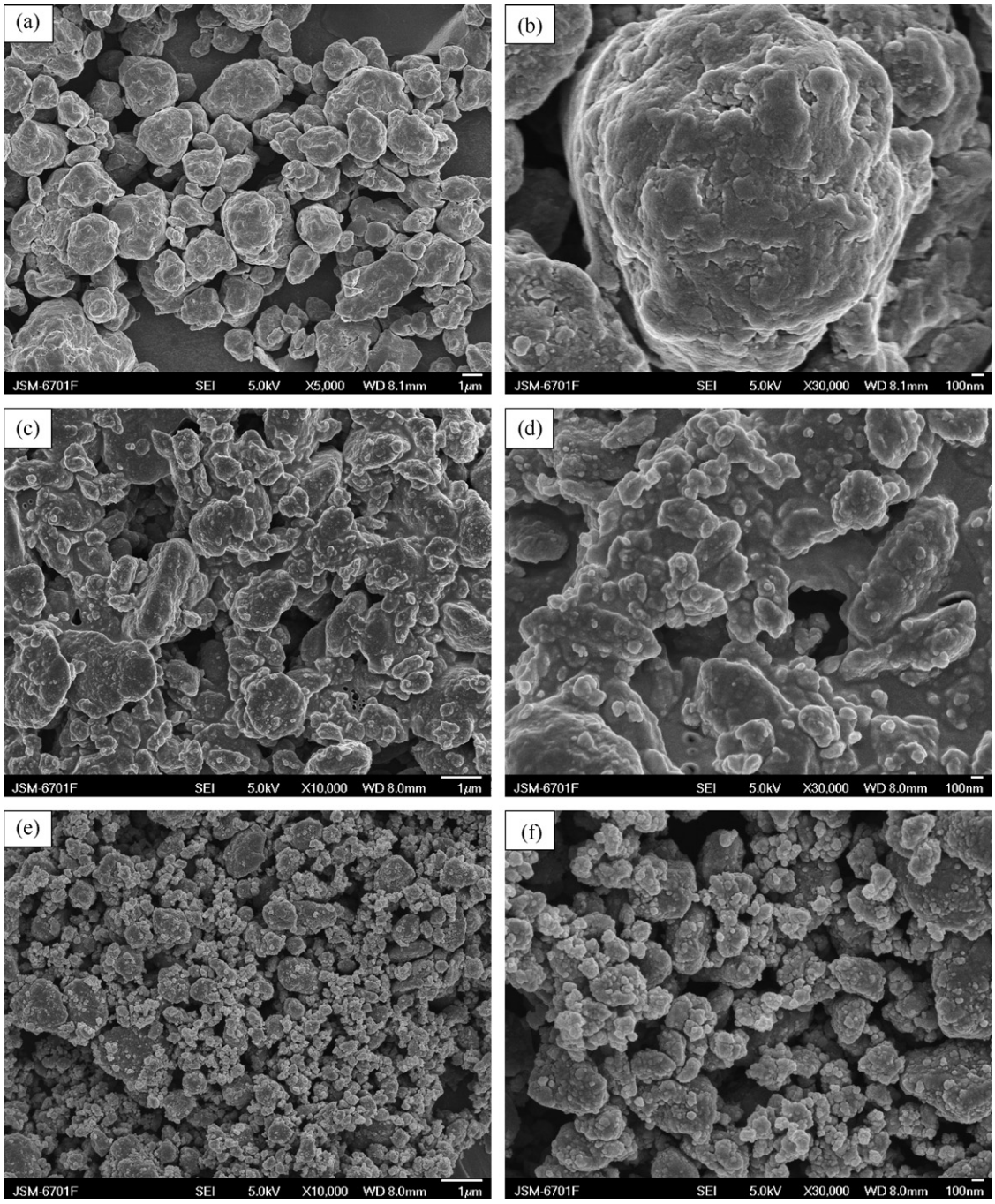

Fig. 3. SEM images of powders collected after milling for (a) and (b) 40 h; (c) and (d) 80 h; (e) and (f) 120 h.

vant XRD data shown in Fig. 2. In other words, the disappearance of Al peaks and the shift of Ni peaks towards lower angles after 40 h of milling well correspond to the significant decrease of the atomic concentration of Al thereafter. This is due to the combination of decreased diffusion distance or interlamellar spacing, increased lattice defect density, and any heating that may have occurred during the milling operation. Thus, with further milling, Al atoms had been dissolved into Ni lattice forming Ni(Al) solid solution. According to the equilibrium diagram, at room temperature Al can be dissolved in Ni lattice up to a maximum atomic concentration of about 5% [30]. Therefore, it can be inferred that a supersaturated Ni(Al) solid solution was formed after 40 h of milling. With further milling, the particles get work hardened and fracture by a fatigue failure mechanism and by the fragmentation of fragile flakes. Fragments generated by this mechanism may continue to reduce in size in the absence of strong agglomerating forces [6]. As shown in Fig. 3c and d, due to the continued impact of grinding balls, the structure of the particles is steadily refined and flake-like particles with an

Table 3
Atomic composition of the powders formed after milling for different time (determined by EDS).

Powders	Atomic composition (at.%)	
	Ni	Al
After 40 h milling	97.06	2.94
After 80 h milling	85.92	14.08
After 120 h milling	72.04	27.96

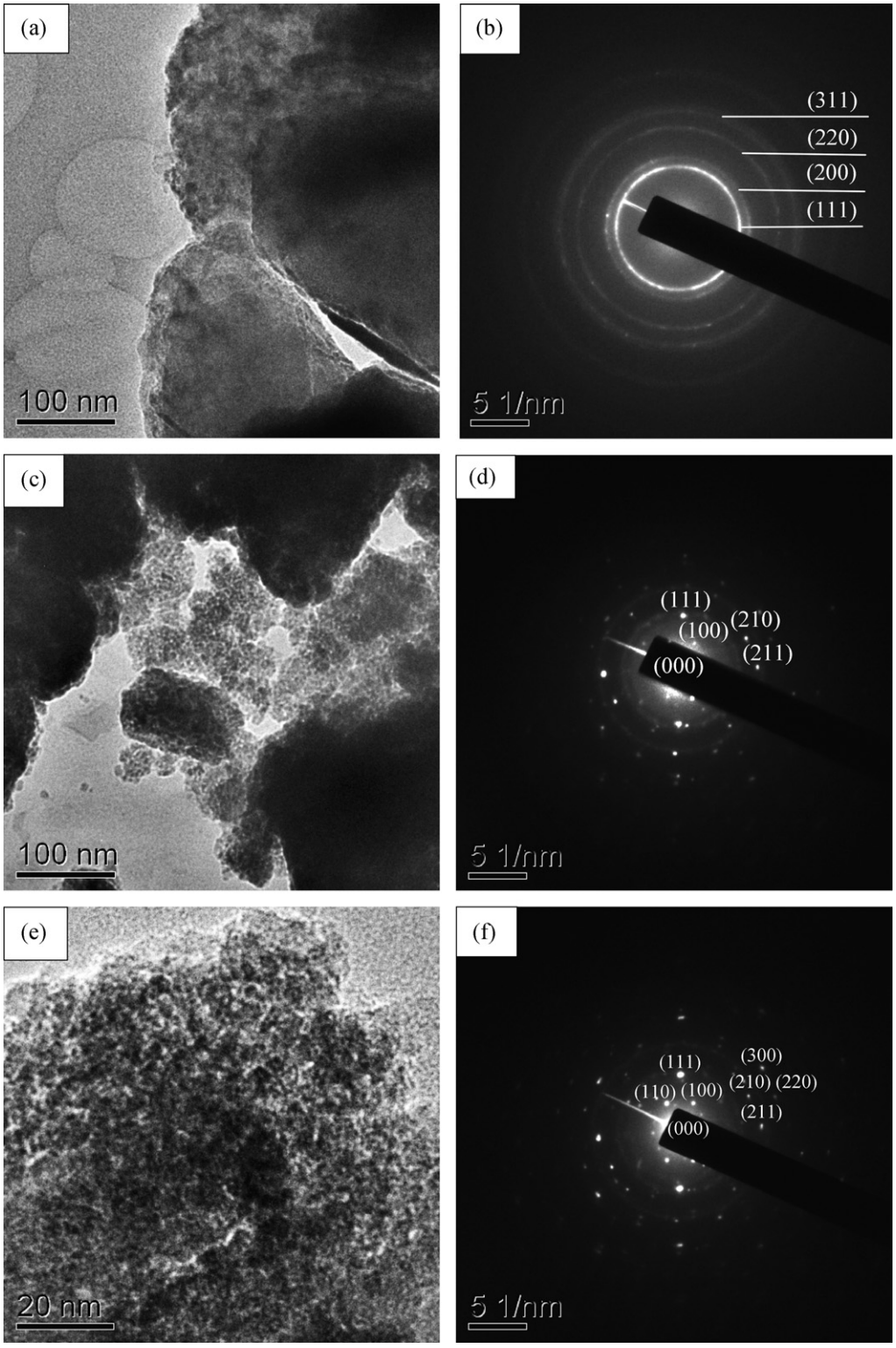

Fig. 4. TEM images and corresponding selected-area diffraction pattern of the powders collected after milling for (a) and (b) 40 h; (c) and (d) 80 h; (e) and (f) 120 h.

average size of about 1 μm were formed after an extended milling time of 80 h. The flakes are composed of nanoparticles with a size of about 150 nm (see Fig. 3d) and have a nominal atomic composition of 85.92% Ni and 14.08% Al determined by using the EDS attached to SEM. Interestingly, extending milling time led to significant decrease of Ni content and obvious increase of Al content of the milled particles, which indicates that supersaturated Ni(Al) solid solution had been transformed into Ni_3Al intermetallic compound via Ni diffusion, because of the accumulation of internal strain and refinement of grains under severe plastic deformation associated with extended milling. Thus it can be inferred that Ni_3Al intermetallic compound was formed after 80 h of milling. When the milling time was further increased to 120 h, equiaxial particles of Ni_3Al intermetallic compound, with nearly uniform size of about 0.5 μm, were obtained (see Fig. 3e and f). The equiaxial particles of Ni_3Al intermetallic compound in this case, composed of nanoparticles

with a size of about 100 nm, have a nominal atomic composition of 72.04% Ni and 27.96% Al, which is close to the stoichiometric composition of Ni_3Al. Therefore, it can be concluded that supersaturated Ni(Al) solid solution had been fully transformed into Ni_3Al intermetallic compound via Ni diffusion after 120 h of milling.

Fig. 4 shows the TEM images and corresponding selected-area electron diffraction (SAED) patterns of the powders collected after 40 h, 80 h, and 120 h of milling. As mentioned above, due to the repeated action of cold welding and fracturing of the powder particles during MA process, Al atoms had been dissolved into Ni lattice and formed the multi-layered structural Ni(Al) solid solution with grain size of about 10–100 nm after 40 h of milling time (see Fig. 4a). The corresponding SAED pattern (see Fig. 4b), the diffraction rings, can be indexed to fcc-Ni. The EDS analysis attached to the TEM (with an electron beam of 3.5 nm) indicates that the nanograins collected after 40 h of milling are composed of supersaturated Ni(Al) solid solution and have a nominal atomic composition of 90.83% Ni and 9.17% Al. Such a nominal atomic composition determined by using the EDS attached to TEM obviously differs from that determined by using the EDS attached to SEM (97.06% Ni, 2.94% Al), which might be attributed to the different spatial resolution of the two types of energy dispersive spectrometer. Moreover, as shown in Fig. 4b, although severe plastic deformation occurred during the milling process, the powders were refined to generate nanograins free of dislocation activity, as what was reported elsewhere [28,31–33]. In other words, it can be concluded that mechanical alloying induced by 40 h of ball milling leads to the formation of nanostructured surpersaturated Ni(Al) solid solution with a grain size of below 100 nm. With further milling, the accumulation of internal strain and refinement of grains during MA process leads to decrease the diffusion distances and increase lattice defect density. Additionally, the slight rise in temperature during milling further aids the diffusion behavior. At an extended milling time of 80 h, the nanostructured supersaturated Ni(Al) solid solution had been transformed into Ni_3Al intermetallic compound with grain size of about 20 nm via Ni diffusion (see Fig. 4c). The corresponding SAED pattern (see Fig. 4d), the diffraction spots can be well indexed to Ni_3Al. Interestingly, the (1 0 0), (2 1 0), and (2 1 1) superlattice reflections of ordered $L1_2$ structure appear in Fig. 4d, which indicates that crystalline Ni_3Al phase formed after 80 h of milling has an ordered structure. Increasing milling time to 120 h resulted in formation of Ni_3Al particles composed of nanograins with a size of about 10 nm (see Fig. 4e), conforming to relevant XRD data. The corresponding SAED pattern (see Fig. 4f), the diffraction spots can be well indexed to Ni_3Al. In this case the analysis using the EDS attached to the TEM verifies that the nanograined Ni_3Al particles have a nominal atomic composition of 73.15% Ni and 26.85% Al. At the same time, the (1 0 0), (1 1 0), (2 1 0), and (2 1 1) superlattice reflections of ordered $L1_2$ structure appear in Fig. 4f, which indicates that crystalline Ni_3Al phase formed after 120 h of milling has an ordered structure. However, these superlattice reflections were not detected in XRD analysis, possibly due to the different spatial resolution of the two types of facilities. Namely, the TEM analysis was carried out at a limit spatial resolution of about 2 μm, while XRD analysis was performed over much larger spatial locations (the diffraction data were collected over a 2θ range of 30–100°). Compared with the other reflections such as (1 1 1) reflection, the intensity of the superlattice reflection is very small and can hardly be detected by XRD. In addition, as mentioned above, surpersaturated Ni(Al) solid solution formed in mechanical alloying process was free of dislocation activity even though nanograin microstructure was formed. And naturally, the supersaturated Ni(Al) solid solution would be readily transformed into ordered Ni_3Al nanocrystalline upon fully extended ball milling.

4. Conclusions

Ni_3Al nanocrystalline was successfully fabricated by mechanical alloying of the mixed powders of elemental Ni and Al. The analyses of XRD, SEM, TEM, and EDS indicate that 40 h of milling led to the formation of supersaturated Ni(Al) solid solution. Upon further milling, the Ni(Al) solid solution was transformed into ordered Ni_3Al intermetallic compound with nanocrystalline structure. Such a transformation is attributed to Ni diffusion in association with the accumulation of internal strain and refinement of grain size under severe plastic deformation. To obtain well ordered Ni_3Al nanocrystallines composed of fine nanograins of a size below 11 nm, it is imperative to realize full transformation of Ni(Al) solid solution into ordered Ni_3Al intermetallic compound by ball milling for an adequately extended time of up to 120 h.

Acknowledgements

The authors wish to acknowledge the financial support from the Ministry of Science and Technology of China (project of “863” Plan, Grant No. 2006AA03A219) and Chinese Academy of Sciences (“The program of the light in west China (2006))”.

References

[1] S.C. Hanyaloglu, B. Aksakal, I.J. McColm, Mater. Charact. 47 (2001) 9–16.
[2] V.K. Portnoy, A.M. Blinov, I.A. Tomilin, V.N. Kuznetsov, T. Kulik, J. Alloys Compd. 336 (2002) 196–201.
[3] S.C. Deevi, V.K. Sikka, C.T. Liu, Prog. Mater. Sci. 42 (1997) 177–192.
[4] S.C. Deevi, V.K. Sikka, Intermetallics 4 (1996) 357–375.
[5] D.P. Pope, S.S. Ezz, Int. Mater. Rev. 29 (1984) 136–167.
[6] C. Suryanarayana, Prog. Mater. Sci. 46 (2001) 1–184.
[7] C.T. Liu, D.P. Pope, in: J.H. Westbrook, R.L. Fleischer (Eds.), Intermetallic Compounds, vol. 2, Wiley, New York, 2000, pp. 17–47.
[8] E.P. George, C.T. Liu, H. Lin, D.P. Pope, Mater. Sci. Eng. A 192–193 (1995) 277–288.
[9] C.T. Liu, C.L. White, J.A. Horton, Acta Metall. 33 (1985) 213–229.
[10] C.T. Liu, J.O. Stiegler, Science 226 (1984) 636–642.
[11] E.P. George, M. Yamaguchi, K.S. Kumar, C.T. Liu, Annu. Rev. Mater. Sci. 24 (1994) 409–451.
[12] S.X. McFadden, R.S. Mishra, R.Z. Valiev, A.P. Zhilyaev, A.K. Mukherjee, Nature 398 (1999) 684–686.
[13] C. Suryanarayana, F.H. Froes, Metall. Trans. A 23 (1992) 1071–1081.
[14] G.W. Nieman, J.R. Weertman, R.W. Siegel, Nanostruct. Mater. 1 (1992) 185–190.
[15] R.W. Siegel, G.E. Fougere, Nanostruct. Mater. 6 (1995) 205–216.
[16] C.C. Koch, J.D. Whittenberger, Intermetallics 4 (1996) 339–355.
[17] M.H. Enayati, F. Karimzadeh, S.Z. Anvari, J. Mater. Process Technol. 200 (2008) 312–315.
[18] S.Z. Anvari, F. Karimzadeh, M.H. Enayati, J. Alloys Compd. 477 (2009) 178–181.
[19] N. Forouzanmehr, F. Karimzadeh, M.H. Enayati, J. Alloys Compd. 478 (2009) 257–259.
[20] F. Cardellini, G. Mazzone, A. Montone, M. Vittori Antisari, Acta Metall. Mater. 42 (1994) 2445–2451.
[21] M.H. Enayati, Z. Sadeghian, M. Salehi, A. Saidi, Mater. Sci. Eng. A 375–377 (2004) 809–811.
[22] M. Krasnowski, A. Antolak, T. Kulik, Rev. Adv. Mater. Sci. 10 (2005) 417–421.
[23] M. Krasnowski, A. Antolak, T. Kulik, J. Alloys Compd. 434–435 (2007) 344–347.
[24] A. Antolak, M. Krasnowski, T. Kulik, Rev. Adv. Mater. Sci. 18 (2008) 384–392.
[25] G.K. Williamson, W.H. Hall, Acta Metall. 1 (1953) 22–31.
[26] H.P. Klug, L.E. Alexander, X-ray Diffraction Procedures for Polycrystalline and Amorphous Materials, John Wiley and Sons, London, 1954.
[27] A.R. Stokes, A.J.C. Wilson, Proc. Phys. Soc. Lond. 56 (1944) 174–181.
[28] L. Shaw, H. Luo, J. Villegas, D. Miracle, Acta Mater. 51 (2003) 2647–2663.
[29] JCPDS PDF card 09-0097.
[30] T.B. Massalski, Binary Phase Diagrams, ASM International, Materials Park, OH, 1986.
[31] A.L. Ortiz, L. Show, Acta Mater. 52 (2004) 2185–2197.
[32] D.G. Morris, M.A. Morris, Acta Metall. Mater. 39 (1991) 1763–1770.
[33] X.K. Sun, H.T. Cong, M. Sun, M.C. Yang, Metall. Mater. Trans. A 31 (2000) 1017–1024.